

# A MODEL FOR A HIGH-POWER SCALING FFAG RING

G. H. Rees, D. J. Kelliher, S. Machida, C. R. Prior, S. L. Sheehy,  
STFC Rutherford Laboratory, ASTeC, UK.

## Abstract

High-power FFAG rings are under study to serve as drivers for neutron spallation, muon production, and accelerator-driven reactor systems. In this paper, which follows on from earlier work [1], a 20 - 70 MeV model for a high-power FFAG driver is described. This model would serve as a test bed to study topics such as space charge and injection in such rings. The design incorporates a long straight to facilitate  $H^-$  charge exchange injection. The dynamic aperture is calculated in order to optimize the working point in tune space. The injection scheme is also described. A separate design for an ISIS injector, featuring a novel modification to the scaling law, was also studied.

## INTRODUCTION

In FFAG accelerators, the repetition rate is in principle limited only by the available rf voltage. Indeed the potential for FFAGs to accelerate high intensity beams was one of the motivations behind their revival in the 2000's in Japan [2],[3]. Space charge studies are planned, making use of the ERIT ring at KURRI, Japan. However, in order to take the study of various aspects of intense proton beams to the next stage, building a dedicated FFAG is required.

## FFAG MODEL

Taking a lead from KURRI, the study takes as its starting point a 100 Hz, 20 MeV,  $H^-$  linac injecting into a 20-70 MeV, FFAG,  $H^+$  ring. An 8 cell DFD lattice is proposed with cell tunes  $\nu_x = 0.401$ ,  $\nu_y = 0.223$  and  $\gamma_t = 2.3368$ . The cell tunes are chosen to avoid principal resonances, but may be adjusted following a dynamic aperture survey. The F and D have opposite field directions, so a "return yoke free magnet" is proposed with magnetic shields to reduce end fields as used at KURRI. The edges of the magnet are radial. Each cell is mirror symmetric about the F centre with long drifts at either end.

Table 1: Lattice Parameters at Injection and Extraction

Parameter	Unit	Injection	Extraction
Short drift length	m	0.178	0.200
Long drift length	m	1.669	1.878
F length	m	1.450	1.632
D length	m	0.217	0.244
D bend angle	rad	- 0.168	-0.168
F bend angle	rad	1.120	1.120
F, D norm. gradient	$m^{-2}$	$\pm 0.541$	$\pm 0.685$
Edge field extent	m	0.034	0.030
Mean radius	m	4.976	5.600

The initial design work was carried out using a matrix code to model each momentum separately. In order to calculate the optics, the magnets are simulated as dipoles with quadrupole component and finite edge angles. The lattice parameters at injection and extraction used in the matrix code are listed in Table 1. In order to pursue further studies such as a calculation of dynamic aperture, the lattice was simulated by the Zgoubi tracking code.

Table 2: Lattice Parameters in Zgoubi Model

Parameter	Unit	Value
Field index	-	4.345
Reference radius $r_0$	m	5.6
D&F Field at $r_0$	T	-1.078, 0.845
D&F radial extent	rad	0.044 , 0.291
Edge field extent	m	0.034

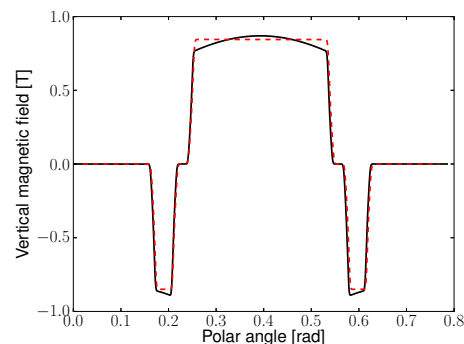


Figure 1: Comparison of vertical magnetic field along the closed orbit at the extraction momentum in one cell between the ASTeC matrix code STRING (black solid) and Zgoubi models (red dash).

In Zgoubi the magnets are simulated as radial FFAGs in which the reference radius  $r_0$ , field  $B_0$ , angular extent and field index  $k$  need to be specified. The field index is given by  $k = g_n * r_m * \rho$  where  $g_n$  is the normalised gradient and  $r_m$  the mean radius at a particular momentum and  $\rho$  is the magnet bending radius. However there are a couple of significant differences between the matrix and Zgoubi models of the magnets.

In the matrix code the curvature of the lines of constant vertical field in the D is in the opposite sense to that in the F and, furthermore, the radius of curvature is equivalent to the bending radius. This ensures that the closed orbit at any momentum corresponds to a line of constant field (excepting the variation due to the end fields). By contrast in

Zgoubi the curvature in the D is in the same sense as the F and the radius of curvature of the field lines is the machine radius. This results in a variation in the field and the gradient along the closed orbit and consequently different cell tunes than in the case of the matrix code. The difference in the field between the two codes is shown at the extraction momentum in Fig. 1.

By adjusting the field index and the D/F field ratio, the desired cell tunes in the tracking code are restored. Following this adjustment, the parameters used in the Zgoubi model are given in Table 2. As a further check of the degree of similarity between the two models from an optical point of view, the horizontal and vertical beta profiles calculated by the matrix and tracking codes are compared in Fig. 2.

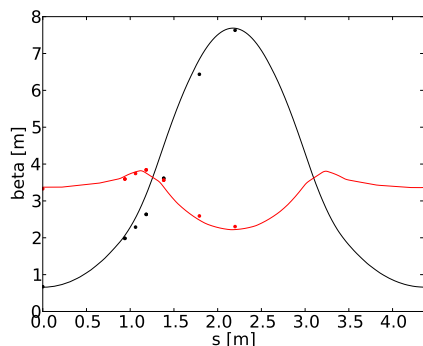


Figure 2: Comparison of beta profile calculated by Zgoubi (solid) with that calculated by the matrix code STRING (dots) in the horizontal (black) and vertical (red) planes.

## DYNAMIC APERTURE

The dynamic aperture of the FFAG is calculated by means of single particle tracking. For each emittance tested, a single particle is chosen from the phase space ellipse. A small amplitude particle is tracked for 500 turns at the injection momentum. The amplitude is increased and the tracking repeated until the motion becomes unstable. The study began by checking the dynamic aperture in the horizontal plane with zero vertical amplitude ( $y = y' = 0$ ) and assuming a lattice free of imperfections. In this case the aperture is  $2500\pi$  mm mrad which is much greater than the  $55\pi$  mm mrad needed for a  $10^{13}$  proton bunch. The aperture appears to be limited by the sextupole-driven resonance at  $\nu_x = 1/3$ . The stable region within the dynamic aperture is shown in Fig. 3.

The calculation is then repeated but now including a vertical amplitude. Equal emittances are assumed in the horizontal and vertical plane at each stage. The dynamic aperture is in this case significantly reduced to  $200\pi$  mm mrad. Detuning with amplitude causes the vertical cell tune to approach  $\nu_y = 0.25$  where it encounters a resonance driven by high order terms such as octupole. The vertical phase space is shown in Fig.4. The dynamic aperture is still more than required but may be reduced further when lattice im-

perfections and space charge effects are included.

As a first step towards establishing the optimal working point, the variation of dynamic aperture with vertical tune was calculated. The scan was limited to the interval  $0.1875 < \nu_y < 0.25$  which, in this 8 cell lattice, is bounded by a half-integer and integer ring tune. The horizontal tune was kept fixed at nominal,  $\nu_x = 0.4$ . From the result of the scan, shown in Fig. 5, it is apparent that the general trend is for the dynamic aperture to decline as  $\nu_y = 0.25$  is approached.

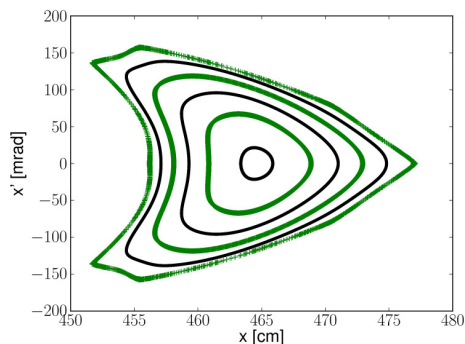


Figure 3: Stable region in horizontal phase space with a zero vertical emittance beam, no lattice imperfections and tracking for 500 turns. The innermost curve shows the required aperture.

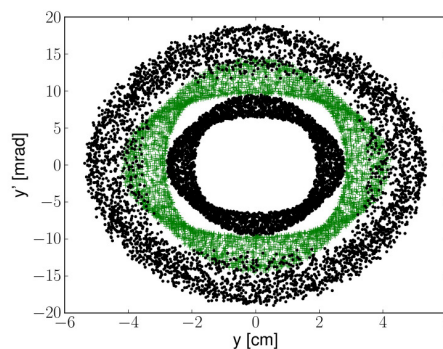


Figure 4: Stable region in vertical phase space with equal emittances in both planes, no lattice imperfections and tracking for 500 turns. The innermost curve shows the required aperture.

## INJECTION

A multi-turn,  $H^-$  injection scheme is considered. The injection straight is too short to house a bump magnet chicane, so the merging of incoming  $H^-$  ions and the recirculating protons has to occur in a lattice cell's bending-focusing region. Since the cells consist of DFD triplets, the proposed  $H^-$  stripping foil location is in a short drift between a D and F magnet within the end field region of the

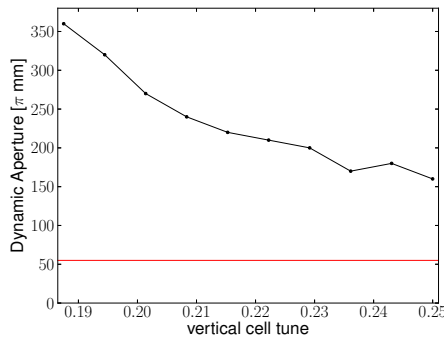


Figure 5: Dynamic aperture variation with vertical cell tune in the range  $0.1875 < \nu_y < 0.25$  with horizontal cell tune fixed at  $\nu_x = 0.4$ . The red line show the required aperture.

D magnet. The field level is chosen so stripped electrons bend to be collected outside the ring’s acceptance.

Figure 6 is a schematic drawing of the proposed injection system. An injection septum magnet is not needed as  $H^-$  ions bend and focus in the opposite sense to protons. The input  $H^-$  beam ( $\sim \pm 10\sigma$ ) is scraped to ( $\sim \pm 5\sigma$ ) in the input line and directed to oscillate about or precisely follow the ring’s closed orbit at the injection momentum. It is directed at a fixed spot on the foil, which is set on the vertical axis. Two steering magnets in the injection line sweep the beam vertically over a range of incident angles. In addition, the betatron phase space painting requires a programmed, collapsing horizontal orbit bump, together with a rf system frequency ramp. The beam centre at the foil is set at ( $\sim \pm 5\sigma$ ) from the adjacent foil corner edges, so negative steering causes some input beam to miss the foil.

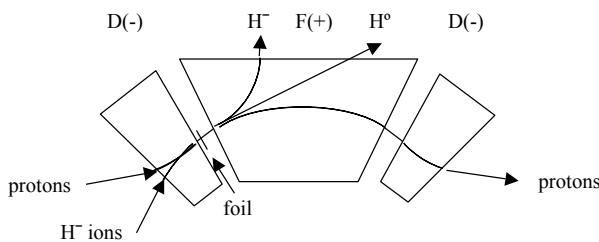


Figure 6: Schematic drawing for the multi-turn injection of  $H^-$  ions.

The horizontal injection orbit bump requires a pair of horizontal steering magnets on each side of the triplet set involved. Unstripped  $H^-$  ions and partially stripped  $H^0$  atoms which remain after the foil, are collected on the outside of the FFAG ring, after passing through the following F magnet as indicated on Fig 6.

### ISIS INJECTOR

A 150 MeV design for a potential ISIS injector was also considered. Its outer radius must be chosen to allow appropriately timed extraction. Assume circumferences  $L$  and

$L/p$  for the ISIS and FFAG rings, where  $p$ , the ratio of two integers, is set by an ejection delay needed for the second bunch after the first ( $n$  more turns in the new ring, and  $m$  more in ISIS). Extraction at the correct instant then requires  $L(1 + 2m) = L(1 + 2n)/p$ . One solution is given by ( $m = 2, n = 6, p = 13/5$ ) which, given that the ISIS mean radius is 26 m, leads to an outer radius in the FFAG of 10.0 m.

A scaling DFD triplet ring with 14 identical cells is proposed. As before, each cell is mirror symmetric about the F centre with 1.924 m drifts at either end. However, in this case the magnets are parallel edged with poles offset relative to one another. Though parallel edges simplify construction, it breaks the scaling condition and leads to some variation in tune with momentum.

A modified scaling field is considered, given by

$$\frac{B}{B_0} = \left(1 + \frac{\alpha x}{r_0}\right)^{K/\alpha} \quad (1)$$

where  $B_0$  is the field on a reference orbit at a distance  $r_0$  from the ring centre and  $x$  is the radial offset from  $r_0$ . The traditional scaling field is obtained by setting  $\alpha = 1$  but choosing  $\alpha \neq 1$  allows the multipole field ratio to be varied. By carefully choosing  $\alpha$ , the variation of the horizontal tune with momentum is minimised. The variation in the vertical tune is reduced by adjusting the end field extents. The effect of  $\alpha$  on the horizontal tune can be seen by comparing Table 3, in which it is zero, to Table 4, in which  $\alpha = 0.957$ .

Table 3: Parameters for the FFAG with  $\alpha=0$

T MeV	$r_0 + x$ m	Q(h)	Q(v)	F extent m
20.0	9.27	5.313	2.402	0.02
55.6	9.63	5.304	2.421	0.06
150	10.0	5.293	2.442	0.1

Table 4: Parameters for the FFAG with  $\alpha=0.957$ .

T MeV	$r_0 + x$ m	Q(h)	Q(v)	F extent m
20.0	9.27	5.312	2.402	0.02
55.6	9.63	5.313	2.419	0.06
150	10.0	5.312	2.438	0.1

### REFERENCES

- [1] G.H. Rees and D.J. Kelliher, “New, high power, scaling, FFAG driver ring designs” HB2010, Morschach, September 2010, MOPD07, p. 54, <http://www.JACoW.org>
- [2] M. Aiba et al, “Development of FFAG proton synchrotron”, Proc. 7th European Particle Accelerator Conf., Vienna, Austria, 26-30 June 2000, pg. 581.
- [3] Y. Mori, Nucl. Instr. Meth. Phys. Res. A562 (2006) 591.